On the electronic, structural and thermodynamic properties of Au supported on α-Fe_2O_3 surfaces and their interaction with CO

Manh-Thuong Nguyen*
The Abdus Salam International Centre for Theoretical Physics, Strada Costiera 11, 34151 Trieste, Italy1

Matteo Farnesi Camellone†
CNR-IOM DEMOCRITOS, Istituto Officina dei Materiali, Consiglio Nazionale delle Ricerche and SISSA Scuola Internazionale di Studi Superiori Avanzati, Via Bonomea 265, I-34136 Trieste, Italy

Ralph Gebauer
The Abdus Salam International Centre for Theoretical Physics, Strada Costiera 11, 34151 Trieste, Italy
(Dated: June 29, 2015)

Extensive *first principles* calculations are carried out to investigate Au monomers and dimers supported on α-Fe_2O_3 (0001) surfaces in terms of structure optimizations, electronic structure analyses and *ab initio* thermodynamics calculations of surface phase diagrams. All computations rely on density functional theory in the generalized gradient approximation (PBE) and account for on-site Coulomb interactions via inclusion of a Hubbard correction (PBE+U). The relative stability of Au monomers/dimers on the stoichiometric termination of α-Fe2O3 (0001) decorated with various vacancies (multiple oxygen vacancies, iron vacancy, mixed iron-oxygen vacancies) has been computed as a function of the oxygen chemical potential. The charge rearrangement induced by Au at the oxide contact is analyzed in detail and discussed. On one hand *ab initio* thermodynamics predicts that under O-rich conditions, structures obtained by replacing a surface Fe atom with a Au atom are thermodynamically stable over a wide range of temperatures. On the other hand *the complex* of a CO molecule on a Au atom substituting surface Fe atoms is thermodynamically stable only in a much more narrow range of values of the O chemical potential under O-rich conditions. In the case of a Au dimer, under O-rich conditions, supported Au atoms at an O-Fe di-vacancy are more stable. However, upon CO adsorption, the complex of a CO molecule and 2 Au atoms located at a single Fe vacancy is more favorable.

I. INTRODUCTION

Although gold is one of the most inert metals, Au clusters supported on metal oxides have been shown to catalyze important chemical reactions such as hydrogenation[1], water gas shift[2], and low-temperature CO oxidation[3]. Among many Au/oxide catalysts, gold nanoparticles prepared in different ways and supported on hematite α-Fe_2O_3 have shown high catalytic activity for CO oxidation even at $-70°C$[4,5,6].

α-Fe_2O_3 is a stable form of iron oxide, it is nontoxic, very abundant in nature, and as a semiconductor with a band gap of 2.0 eV, is employed in several (photo-)catalytic processes. Au/hematite catalysts have been studied for more than two decades[4,7,8,9,10,11,12,13,14], employing different experimental techniques such as X-ray photoelectron spectroscopy[4,11] or Fourier transform infrared spectroscopy[9]. However, little is known about the active sites and the microscopic mechanisms of chemical reactions such as CO oxidation on hematite supported Au nanoparticles.

From a theoretical perspective, the understanding of metal oxide supported Au systems such as Au/TiO_2[15] or Au/CeO_2[16] is well achieved, theoretical insights into Au/Fe_2O_3 systems are still missing. In this study we have have carried out extensive density functional based calculations to better understand the the geometric and electronic properties of Au atoms supported or dispersed on hematite surfaces, and their interaction with CO. We focus on the single iron terminated α-Fe_2O_3 (0001) surface that represents one of the natural growth faces of hematite[17] and has been well studied. It is the most thermodynamically stable surface in a wide range of temperatures and pressures that are relevant for applications in the realm of catalysis[18,19]. Both defect-free and defective hematite surfaces have been modeled since defects are unavoidable and stable on these substrates under particular environmental conditions[18].

II. METHODOLOGY AND MODELS

The spin-polarized Kohn-Sham equations were solved in the plane-wave and pseudopotential frameworks using Vanderbilt's ultrasoft pseudopotentials[20] as implemented in the quantum-ESPRESSO code[21]. The gradient-corrected Perdew-Burke-Ernzerhof functional (PBE)[22] was employed to describe semilocally the exchange-correlation effects. It is well established that adding a Hubbard U term[23] acting on the Fe *3*d states in Fe_2O_3

orbitals greatly improves the quality of LDA or GGAs in describing the electronic structure of both oxidized and reduced hematite surfaces. In line with our previous work[19], the value of U = 4.2 eV was adopted. A kinetic energy cutoff of 40 Ry for the wavefunction and 400 Ry for the charge density has been employed. The charge transfer at the metal-oxide interface has been quantified by means of Bader's theory of atoms in molecules [24,25]. The single iron terminated $Fe_2O_3(0001)$ surfaces have been modeled by approximately 3 oxygen-iron double-layers (56 atoms) 2×2 supercell slabs separated by more than 20 Å (see Fig. 1). All structures were relaxed by minimizing the atomic forces, where convergence was assumed to have been achieved when the maximum component of the residual forces on the ions was less than 0.001 a.u. Here, the lowest double-layer atoms (20 in total) were constrained to their bulk positions while all other atoms were free to move during optimization. We have employed a $2 \times 2 \times 1$ k-point grid to sample the Brillouin zone in geometry relaxations, whereas a denser k-point mesh $3 \times 3 \times 1$ grid was used for post processing.

We define the binding energy of Au on Fe_2O_3 surfaces as

$$\Delta E_{\rm Au} = \frac{1}{n_{\rm Au}}[E_{\rm Au/V_{O,Fe}-surf} - E_{\rm V_{O,Fe}-surf} - n_{\rm Au}\mu_{\rm Au}], \quad (1)$$

where $E_{\rm Au/V_{O,Fe}-suf}$, $E_{\rm V_{O,Fe}-surf}$, and $\mu_{\rm Au}$ are the energy of the Au atom located at vacancy sites of the surface, the energy of vacancy surfaces and chemical potential of Au atom which is given below, respectively, and $n_{\rm Au}$ is the number of Au atoms.

The effect of temperature and pressure on the relative stability of the $Au/Fe_2O_3(0001)$ surface structures has been studied by employing the so-called *a*b initio thermodynamics approach.

The adsorption free energy per Au atom on $Fe_2O_3(0001)$ surfaces $\Delta G_{\rm Au}(T,p)$ is assumed to depend on the temperature and pressure only via the oxygen chemical potential $\mu_{\rm O}$ given by

$$\mu_{\rm O} = \frac{1}{2}[E_{\rm O_2} + \tilde{\mu}_{\rm O_2}(T,p^0) + k_{\rm B}T\ln(\frac{p_{\rm O_2}}{p^0})], \quad (2)$$

which represents the thermodynamic reservoir for the O_2 environment that is in contact with the surface under consideration. Vibrational and rotational entropic contributions to $\mu_{\rm O}(T,p)$ at 1 atm are included through the term $\tilde{\mu}_{\rm O_2}(T,p^0)$ by means of thermodynamic tables[26,27]. To avoid inaccurate PBE energy calculations of the O_2 molecule, its energy value is determined using that of H_2 and H_2O molecules, namely the free energy change of $2H_2O \rightarrow 2H_2 + O_2$[28]. Under these assumptions and neglecting entropic contributions of the solids involved, the adsorption free energy per Au atom as a function of pressure and temperature assumes the expression[29]

$$\Delta G_{\rm Au} = \frac{1}{n_{\rm Au}}[E_{\rm Au/V_{O,Fe-surf}} + n_{\rm V_O}\mu_{\rm O} + n_{\rm V_{Fe}}\mu_{\rm Fe} - E_{\rm surf} - n_{\rm Au}\mu_{\rm Au}], \quad (3)$$

where $\mu_{\rm Fe}$ and $\mu_{\rm Au}$ are the chemical potential of Fe and Au, respectively. The quantities $n_{\rm V_O}$ and $n_{\rm V_{Fe}}$ represent the number of O or Fe vacancies, whereas $n_{\rm Au}$, is the number of Au atoms that are present in the structure under consideration. The terms $E_{\rm Au/V_{O,Fe-surf}}$ and $E_{\rm surf}$ are the total energies of the slab with $n_{\rm Au}$ Au adatoms and decorated by defects consisting of $n_{\rm V_O}$ and $n_{\rm V_{Fe}}$ vacancies, and of the stoichiometric slab, which we take as reference, respectively. In thermodynamic equilibrium the two chemical potentials $\mu_{\rm Fe}$ and $\mu_{\rm O}$ can not be varied independently, and are related by

$$\mu_{\rm Fe} = \frac{1}{2}[\mu_{\rm Fe_2O_3} - 3\mu_{\rm O}], \quad (4)$$

where $\mu_{\rm Fe_2O_3}$ is the chemical potential of hematite per formula unit, set as the total energy per formula unit of the $Fe_2O_3(0001)$ crystal. Finally, the chemical potential of Au, $\mu_{\rm Au}$, is set to be the total energy per atom of the bulk Au fcc crystal.

The binding energy of a CO molecule with a hematite-supported Au system was calculated as

$$\Delta E_{\rm CO} = E_{\rm CO-Au/Fe_2O_3} - E_{\rm CO} - E_{\rm Au/Fe_2O_3}, \quad (5)$$

where $E_{\rm CO-Au/Fe_2O_3}$, $E_{\rm CO}$, and $E_{\rm Au/Fe_2O_3}$ are the total energies of the combined system, of a CO molecule in the gas phase, and of the $Au/Fe_2O_3(0001)$ substrate, respectively.

Eqn. (4) allows us to rewrite the adsorption free energy $\Delta G_{\rm Au}$, Eq. 3, as

$$\Delta G_{\rm Au} = \frac{1}{n_{\rm Au}}[E_{\rm Au/V_{O,Fe-surf}} + (n_{\rm V_O} - \tfrac{3}{2}n_{\rm V_{Fe}})\mu_{\rm O} + \tfrac{1}{2}n_{\rm V_{Fe}}\mu_{\rm Fe_2O_3} - E_{\rm surf} - n_{\rm Au}\mu_{\rm Au}]. \quad (6)$$

Therefore, the energy cost for the formation of surface defects is taken into account via the chemical potential of O atoms and of bulk Fe_2O_3.

Finally, we determine the stability of a CO molecule on various supported Au structures by calculating its adsorption free energy

$$\Delta G_{\rm CO-Au} = E_{\rm CO-Au/V_{O,Fe}-surf} + (n_{\rm V_O} - \tfrac{3}{2}n_{\rm V_{Fe}})\mu_{\rm O} + \tfrac{1}{2}n_{\rm V_{Fe}}\mu_{\rm Fe_2O_3} - E_{\rm surf} - n_{\rm Au}\mu_{\rm Au} - \mu_{\rm CO} \quad (7)$$

Here, $\mu_{\rm CO}$ is the chemical potential of CO. Since $\Delta G_{\rm CO-Au}$ for all supported Au systems has the same dependence on $\mu_{\rm CO}$, for simplicity, we will only consider $\mu_{\rm CO} = E_{\rm CO}$.

III. RESULTS

In the present study, we focus on the structural, electronic and thermodynamic properties of Au monomers and dimers adsorbed or dispersed on stoichiometric or defective $Fe_2O_3(0001)$ surfaces decorated with Fe and O vacancies ($n_{\rm Fe} = 0, 1$ and $n_{\rm O} = 0, 1, 2$). In a second step, we investigate the interaction of selected $Au/Fe_2O_3(0001)$ nanocatalysts with CO molecules, relevant to catalysis.

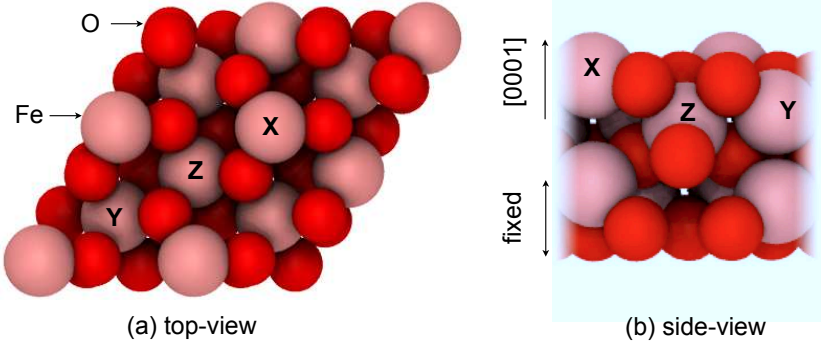

FIG. 1. (a) the 2×2 surface unit cell is indicated by arrows, O atoms are in red and Fe atoms are in pink. **The top-view shows the toichiometric termination of (0001) hematite. The surface area for each unit cell is 90.7 Å^2** (b) Iron atoms in the outermost layer marked with X, in the second layer with Y and Z. Atoms are shown in the relaxed geometry.

A. Thermodynamics

We first discuss the effects of temperature and pressure on the relative stability of Au monomers and dimers on $Fe_2O_3(0001)$ metal/oxide surfaces by employing the formalism of approximate *ab initio* thermodynamics. To this end, we compute the free energies of Au adsorption, $\Delta G_{\rm Au}$ as given by Eq. (6), and report them as a function of the O chemical potential. These free energies are measured relative to the stoichiometric surface and therefore include the free energy cost of creating whatever vacancy the gold atom may be associated with.

Au monomers: Fig. 2 (a) shows the geometries of the most stable adsorption sites of a single Au adatom on stoichiometric and defective $Fe_2O_3(0001)$ surfaces. The corresponding free energies of Au adsorption, $\Delta G_{\rm Au}$ are depicted in Fig. 2 (b) plotted as a function of the effective O chemical potential $\Delta\mu_{\rm O}$. As highlighted in this figure, it is possible to identify three thermodynamically stable phases. The first phase, which holds for values of $\Delta\mu_{\rm O} > 0.8$ eV corresponds to the scenario where a surface Fe atom is replaced by a Au atom. This phase results to be the thermodynamically most stable one under oxidative environments. In a tiny range of oxygen chemical potential $-0.9 > \Delta\mu_{\rm O} > -0.8$ (eV), the structure in which Au replaces Fe in a mixed iron-oxygen divacancy is more stable. The third most stable structure thermodynamically is the one obtained adsorbing an Au atom on a surface $V_{\rm Fe}2V_{\rm O}$ trivacancy. This structure becomes thermodynamically stable for $\Delta\mu_{\rm O} < -1.1$ eV. It turns out that the Au@$V_{\rm Fe}$ structure, is thermodynamically stable in a relatively wide range of temperatures T and pressures p that are relevant for applications in the realm of catalysis, as indicated in Fig. 2(b), the $\Delta\mu_{\rm O} > -0.8$ eV where $200 < T < 300$ (K) and $10^{-35} < p < 10^{10}$ (atm).

Quite interestingly, the adsorption of Au adatoms on the stoichiometric $Fe_2O_3(0001)$ surface is never thermodynamically stable, irrespective of the site where the Au is adsorbed. Three different sites for Au adsorption have been considered on the clean surface. These sites are shown in Fig. 1, and denoted with X, Y and Z. Our calculations suggest that the lowest energy configuration is the one where an Au atom is adsorbed on the site X, followed by sites Y and Z, which are 0.5 and 0.2 eV higher in energy, respectively.

Au dimers: Let us now discuss the phase diagram of Au dimers interacting with stoichiometric and defective $Fe_2O_3(0001)$ surfaces. Fig. 3 (a) shows the geometries of the most stable adsorption sites, while the corresponding adsorption free energies of Au dimers, $\Delta G_{\rm Au}$, are shown in panel c) of the same figure. Here, it is possible to identify three thermodynamically stable phases. The first phase, which holds for values of $\mu_{\rm O} > -0.95$ eV corresponds to an Au dimer adsorbed on the $V_{\rm Fe}V_{\rm O}$ divacancy. The second most stable structure thermodynamically is the one where Au dimers are adsorbed on the stoichiometric $Fe_2O_3(0001)$ surface, and it is stable for $-1.71 < \mu_{\rm O} < -0.95$ (eV) . Finally, at extremely O-poor conditions, namely for $\mu_{\rm O} < -1.71$ eV, Au dimers adsorbed on O divacancy represent the most stable structure thermodynamically.

B. Geometric and electronic properties

Having established which are the most stable Au/$Fe_2O_3(0001)$ structures thermodynamically in a wide range of temperatures and pressures that are relevant for applications in the realm of catalysis, we now discuss in detail their structural and electronic properties. First, we consider Au monomers adsorbed or dispersed on hematite surfaces. As shown in the previous section, Au monomers adsorbed on the stoichiometric $Fe_2O_3(0001)$ surface are never stable thermodynamically. Nevertheless, their structural and electronic properties will be discussed here and used as reference in the following. We note in passing that the transition from these structures to the ones predicted to be the most stable, such as a surface Fe atom replaced by a Au atom, require to overcome energy barriers which are beyond the scope of the present work. To distinguish Au monomers from Au dimers once

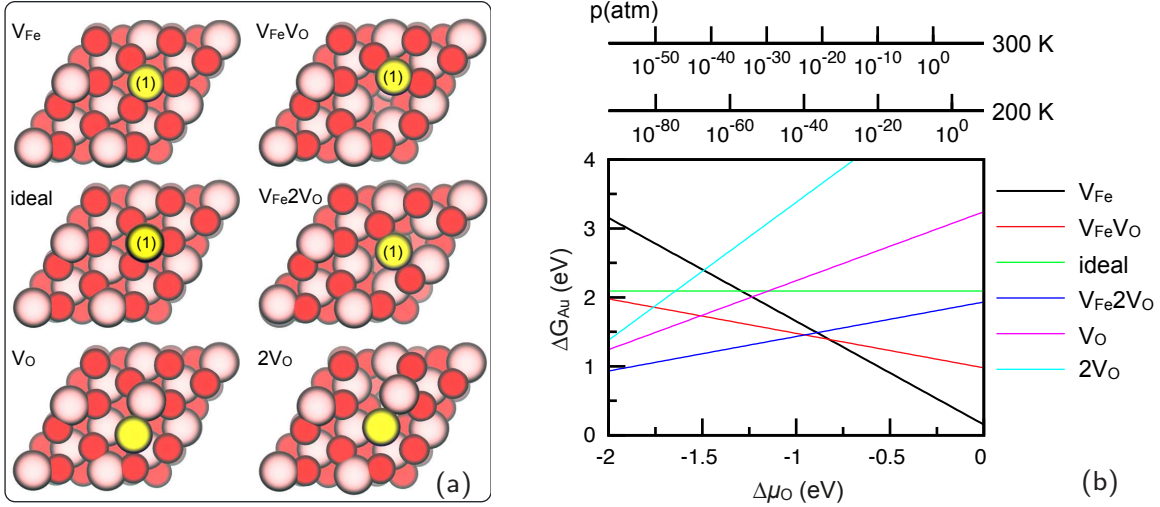

FIG. 2. (a) Gold monomer at hematite surfaces; (b) adsorption free energy of a Au atom against the effective oxygen chemical potential, $\Delta\mu_O = \mu_O - E_{O_2}/2$.

adsorbed or dispersed on the $Fe_2O_3(0001)$ surface, we chose to label Au monomers as 1, whereas a label 2 is assigned to Au atoms added to the surface to create a dimer, as shown in Fig. 3(a).

TABLE I. Bader charges q_{Au}, the $5d$ band center ϵ_d, and the $5d$ band width W_d of adsorbed Au atoms supported on ideal and modified surfaces. ΔE_{Au} is the binding energy of Au on hematite surfaces, in the dimeric cases (indicated by index d), ΔE_{Au} is the average binding energy.

Atom, system	$q_{Au}(\lvert e^-\rvert)$	ϵ_d (eV)	W_d (eV)	ΔE_{Au} (eV)
$Au_m(1)$@ideal	−0.23	−1.4	1.6	+2.09
$Au_m(1)$@V_{Fe}	+1.04	−3.6	4.9	−1.02
$Au_m(1)$@$V_{Fe}V_O$	+0.67	−3.2	4.0	−0.23
$Au_m(1)$@$V_{Fe}2V_O$	+0.40	−3.1	3.7	+0.49
$Au_d(1)$@ideal	−0.24	−2.3	2.5	+1.14
$Au_d(2)$@ideal	+0.25	−2.3	2.8	+1.14
$Au_d(1)$@V_{Fe}	+0.95	−3.8	4.7	+0.39
$Au_d(2)$@V_{Fe}	+0.37	−2.8	3.1	+0.39
$Au_d(1)$@$V_{Fe}V_O$	+0.70	−3.5	4.3	+0.29
$Au_d(2)$@$V_{Fe}V_O$	+0.18	−3.0	3.4	+0.29
$Au_d(1)$@$V_{Fe}2V_O$	+0.25	−2.5	3.1	+0.9
$Au_d(2)$@$V_{Fe}2V_O$	−0.02	−2.9	3.3	+0.9

Au monomers

The most stable adsorption site for a single Au atom adsorbed on the stoichiometric $Fe_2O_3(0001)$ surface is the X site, where the Au atom is on top of a surface Fe atom in the outermost layer, see Fig. 1. The calculations predict a Au(1) − Fe distance of 2.49 Å, in very good agreement (2.5 Å) with a recent DFT+U work[30] where a periodically repeated 1×1 slab was employed. The adsorption of an Au atom on top of a surface Fe site entails a charge rearrangement at the Au/oxide contact. Using Bader charge analyses we can evaluate the charge transfer between Au and Fe_2O_3 by considering the change of partial atomic charge of Au upon adsorption. Our computed results reveals that charge is transferred from the substrate to the adsorbed metal adatom, leading to a a negatively charged $Au^{\delta-}$ species. The magnitude of the charge transfer is 0.23 $|e|$, in quantitative agreement (0.17 $|e|$) with previous work[30].

In contrast, when a surface Fe atom (V_{Fe} site) of the $Fe_2O_3(0001)$ nanocatalyst is replaced by a Au atom, the charge transfer occurs from the metal to the substrate. In this case, the magnitude of the charge transfer, 1.04 $|e|$, is more significant. **The charge redistribution, $\Delta\rho = \rho(\text{Au} - \text{hematite}) - \rho(\text{hematite}) - \rho(\text{Au})$ where $\rho(\text{A})$ is the electron density of system A, in this case can clearly be seen in Fig. 4 (a). A large charge depletion around the Au atom implies a loss of electron of Au to surrounding atoms.** As a result this process leads to the formation of a positively charged $Au^{\delta+}$ species. In this configuration, the computed Au(1)-O bond length is 1.99 Å, and the corresponding binding energy is −1.02 eV. It has been shown in the previous section that this structure is the most thermodynamically stable one under O-rich conditions and in a wide range of the O chemical potential μ_O (see Fig. 2(b)). When one of three O atoms bonded to the Au atom is removed, leading to a $V_{Fe}V_O$ divacancy, the Au atom reduces and its Bader partial atomic charge is 0.67 $|e^-|$. Our calculations suggest that the Au_1-O bond length is slightly shortened by 0.06 Å in this case, see Fig. 2(a). Finally, if a second O atom bonded to the Au atom is removed, thus giving rise to a trivacancy $V_{Fe}2V_O$, the Bader charge analysis reveals that the metal atom has now a net charge of 0.40 $|e^-|$, whereas the a Au(1)-O bond length is 2.02 Å, see Fig. 2(a). In this configuration, the Au atom is also bonded with a not fully oxygen-coordinated Fe atom, and the Au-Fe bond length is 2.84 Å.

It is clear that charge transfer can occur from substrate

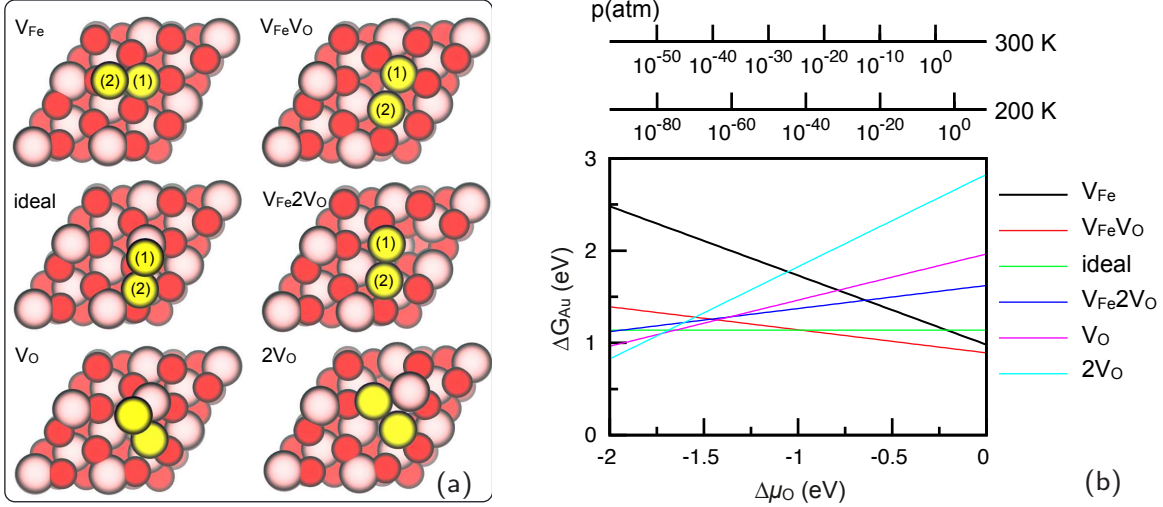

FIG. 3. (a) Gold dimers on hematite surfaces; (b) adsorption free energy per Au atom against the effective oxygen chemical potential, $\Delta\mu_O = \mu_O - E_{O_2}/2$.

to metal or in the opposite direction. The different behaviours can be traced back to the difference in the electronegativity of elements involved. The electronegativity of Fe, Au, and O are 1.83, 1.93, and 3.44, respectively. When the Au atom is adsorbed on the stoichiometric $Fe_2O_3(0001)$ surface (X site) or when it substitutes a surface O atom, it tends to gain electrons, being more electronegative that Fe. In contrast, when the Au atom is bonded to O atoms, it tends to lose electrons, being less electronegative than O. This is in line with our previous findings on Al atoms adsorbed or substituted on $Fe_2O_3(0001)$ surfaces[18], where Al atoms with an electronegativity of 1.61 donates about 1.4 $|e|$ to the surface. The same happens on the $Au/CeO_2(111)$[16], where once adsorbed on top of surface Ce atoms Au atoms lose charge and become positively charged. In this case the electronegativity of Ce is 1.12, therefore lower with respect to the one of Au.

To provide more insights into electronic properties of the most thermodynamically stable $Au/Fe_2O_3(0001)$ systems, we have computed the position of the $5d$-band center,

$$\epsilon_d = \frac{\int_{-\infty}^{\infty} \rho_d(E) E dE}{\int_{-\infty}^{\infty} \rho_d(E) dE}, \tag{8}$$

and the width of the $5d$ band,

$$W_d = \left[\frac{\int_{-\infty}^{\infty} \rho_d(E) E^2 dE}{\int_{-\infty}^{\infty} \rho_d(E) dE} \right]^{1/2}. \tag{9}$$

Fig. 5 (a-d) shows the PDOS of Au monomers in the case of Au adsorbed on the stoichiometric and on defective $Fe_2O_3(0001)$ surfaces. The Au orbitals present different properties depending on their adsorption site. It turns out that when adsorbed on the stoichiometric hematite surface (site X), the Au $5d$ orbitals are only slightly perturbed by the surface environment with a W_d value of 1.6 eV (retaining an atomic-like character), and sitting well below the Fermi level, while the $6s$ states are strongly spin polarized. Half of spin-up and part of the spin-down $6s$ states are unoccupied, implying that Au donates electrons to the surface. The magnetic moment of the Au atom is 0.07 μ_B. The scenario changes when a surface Fe atom is replaced by a Au atom, V_{Fe}. Here, the Au-$5d$ orbitals strongly interact with the neighboring surface atoms. These orbitals appear to be largely broadened, leading to a W_d of 4.9 eV. Some spin-up $5d$ levels are shifted above the Fermi level and become empty, Fig. 5 b), suggesting that electrons are transferred from the metal to the oxide. The magnetic moment of the substitutional Au atom is now 0.6 μ_B, **as visualized with the spin-density in Fig. 4(b)** . When adsorbed at the $V_{Fe}V_O$ divacancy, Au $5d$ orbitals result to be less broadened if compared to the V_{Fe} case, W_d being 4.0 eV, see Fig. 5 c). Nevertheless, the spin-down $5d$ states are still clearly partly unoccupied, and the Au atom carries a 0.26 μ_B dipole moment. Finally, in the trivacancy case $V_{Fe}2V_O$, our calculations suggest that most of the Au $5d$ states are occupied, and the band with slightly narrowed. A relatively small dipole moment of 0.12 μ_B is found on the Au atom. Note that, as listed in Table I, the Au monomers is more stabilized (indicated by the binding energy ΔE_{Au}) when ϵ_d is more negative. Taking the average of ϵ_d of Au(1) and Au(2), this correlation almost holds in the case of Au dimers.

Au dimers: We now turn our attention to Au dimers adsorbed or substituted on the oxide surface. The most stable configurations have been determined adding a second Au atom on the hematite surfaces as discussed in the previous section. We refer to Au(1) and Au(2) when discussing the properties of the two distinct gold atoms forming the dimer. We start by discussing the dimer on the stoichiometric $Fe_2O_3(0001)$ surface.

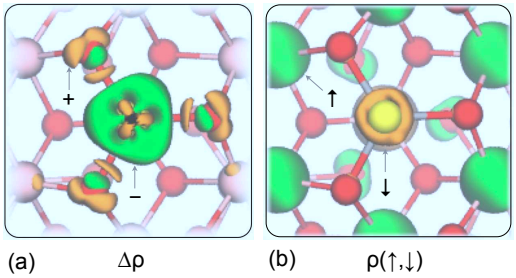

FIG. 4. **(a) Induced charge (iso-surface value set at 0.01 a.u, accumulation in orange, depletion in green) and (b) spin density (iso-surface value set at 0.05 a.u, spin up in green and spin down in orange) of Au@V_{Fe}.**

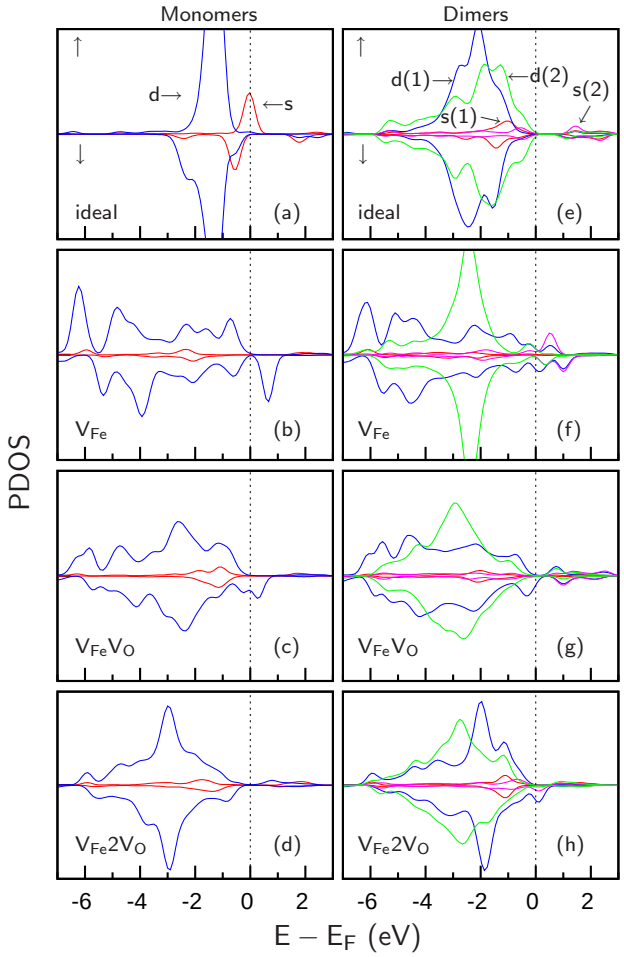

FIG. 5. PDOS (d and s channels) of adsorbed Au atoms in monomer and dimer cases.

Our calculations suggest that the Au(1)-Fe distance is now is 2.66 Å thus larger than the monomer case (2.49Å), whereas the Au(1)-Au(2) distance results to be 2.56 Å. The Bader charge analysis reveals that the Au_1 atom accepts 0.24 electrons resulting in a negatively charged state $Au(1)^{\delta-}$, while the Au(2) atom loses +0.25 $|e^-|$, acquiring a positively charged state $Au(2)^{\delta+}$. In this configuration the Au(2) binds to a surface O atom. Interestingly, it is found that the total charge of the Au dimer is almost zero. The adsorption of an Au dimer on a surface Fe vacancy V_{Fe} leads to a configuration where the Au(1)-O bonds are slightly elongated by 0.01 Å, the Au(1)-Au(2) distance being 2.64 Å, see Fig.3(a). Here, the metal atoms belonging to the Au dimer result to be positively charged, the Au(1) and Au(2) Bader charges being 0.95 $|e^-|$, and 0.37 $|e^-|$, respectively. When adsorbed on the surface with a $V_{Fe}V_O$ divacancy, we find that the Au(1)-O and Au(1)-Au(2) are 1.97 Åand 2.58 Å, respectively. The charges on Au(1) is somewhat more positive (+0.70 $|e^-|$), Au(2) being less charged (+0.18 $|e^-|$) as it is also coordinated with two iron atoms. Finally, on the $V_{Fe}2V_O$ surface the Au_1-O and Au_1-Au_2 bonds results to be 2.0 and 2.5 Å, respectively, whereas the charges on Au(1) is +0.25 $|e^-|$ which is notably smaller than that of +0.4 $|e^-|$ in the monomer case. The charge on Au(2) is almost uncharged in this system.

The PDOS in Fig. 5(e-h) shows significant differences in electronic states between Au(1) and Au(2) in the same system. On the defect-free surface, the 5*d* band of these atoms is much broader than in the monomer system (2.8 vs 1.6 eV). The Au(2) atom is oxygen-bonded, some of its 5*d* and 6*s* states are occupied. Au(1) and Au(2) are slightly spin-polarized by 0.09 and 0.05 μ_B, respectively.

C. CO adsorption

In this section we investigate the adsorption of CO on selected hematite-supported Au structures. The binding energies, first calculated using Eqn. 5, are compiled in Table II. In all cases, supported Au species are clearly more reactive to CO than the bare Fe_2O_3 surface, with binding energies of at least 0.33 eV more favorable [in the case of Au dimer at $V_{Fe}V_O$, CO will binds to $Au_d(2)$].

Note that the Au@hematite composition is dependent on the oxygen chemical potential. We now evaluate the stability of the CO-Au complex by calculating its adsorption free energy, using Eqn. (7).

Monomer: Fig. 6(a) shows the adsorption free energy of the CO-Au complex in different cases. Under O-rich conditions, the CO-Au complex on the V_{Fe} surface is the most stable, whereas under O-poor conditions, the CO-Au complex on the $V_{Fe}2V_O$ surface is more energetically

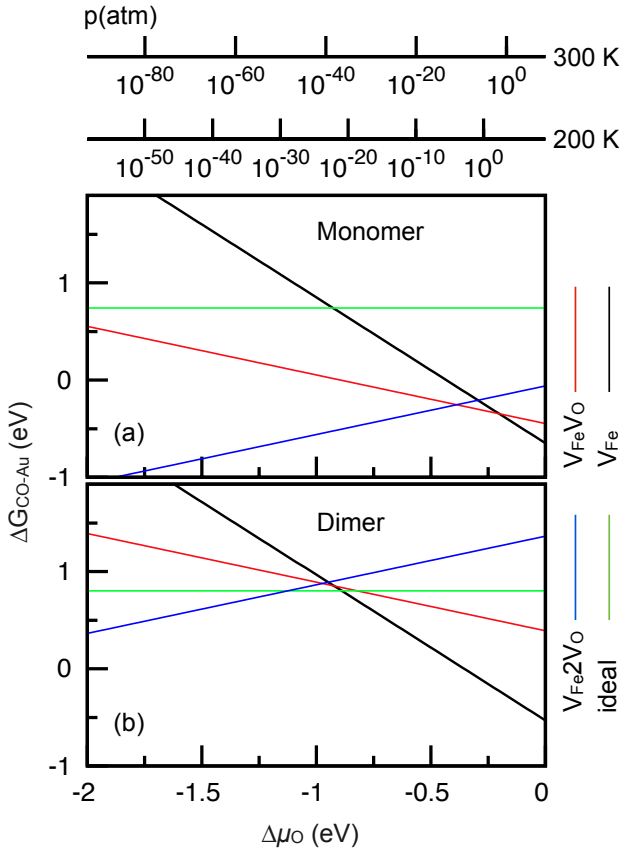

FIG. 6. Adsorption free energy of the CO-Au complex on hematite surfaces, at μ_{CO}=E_{CO}.

favorable.

We now analyze the CO-Au@V_{Fe} structure, see Fig. 7(a). Upon CO adsorption, a Au(1)-O bond is 1.96 Å, and the other two Au(1)-O bonds are 2.8 Å. The adsorbed CO molecule is tilted by 29.5° with respect to the surface normal, the C-O bond length is 1.15 Å, almost unchanged with respect to its gas-phase value of 1.14 Å. The Au-C bond is 1.85 Å. Bader analysis predicts an almost zero charge transfer to CO (0.06 e^-) while the charge on the Au atom now +0.71 $|e^-|$ (note that it is +1.04 $|e^-|$ before CO is introduced). This implies that surrounding surface atoms donate electrons back to Au. In agreement with this, the PDOS on this Au atom, plotted in Fig. 5(b) and 7 (b), clearly shows that upon CO adsorption, unoccupied Au-5*d* states are shifted down to a lower energy region and become occupied.

The W_d value of Au in this CO-Au complex is 4.1 eV, comparing to its initial value of 4.9 eV, showing that the 5*d* states become less dispersed, induced by the interaction with CO.

TABLE II. Binding energy of a CO molecule on hematite-supported Au.

Atom, system	ΔE_{CO}(eV)
ideal	−0.48
$Au_m(1)$@ideal	−1.22
$Au_m(1)$@V_{Fe}	−0.81
$Au_m(1)$@$V_{Fe}V_O$	−1.43
$Au_m(1)$@$V_{Fe}2V_O$	−2.00
$Au_d(1)$@ideal	−1.00
$Au_d(2)$@ideal	−1.47
$Au_d(1)$@V_{Fe}	−1.30
$Au_d(2)$@V_{Fe}	−2.49
$Au_d(1)$@$V_{Fe}V_O$	−0.01
$Au_d(2)$@$V_{Fe}V_O$	−1.39
$Au_d(1)$@$V_{Fe}2V_O$	−1.88
$Au_d(2)$@$V_{Fe}2V_O$	−1.61

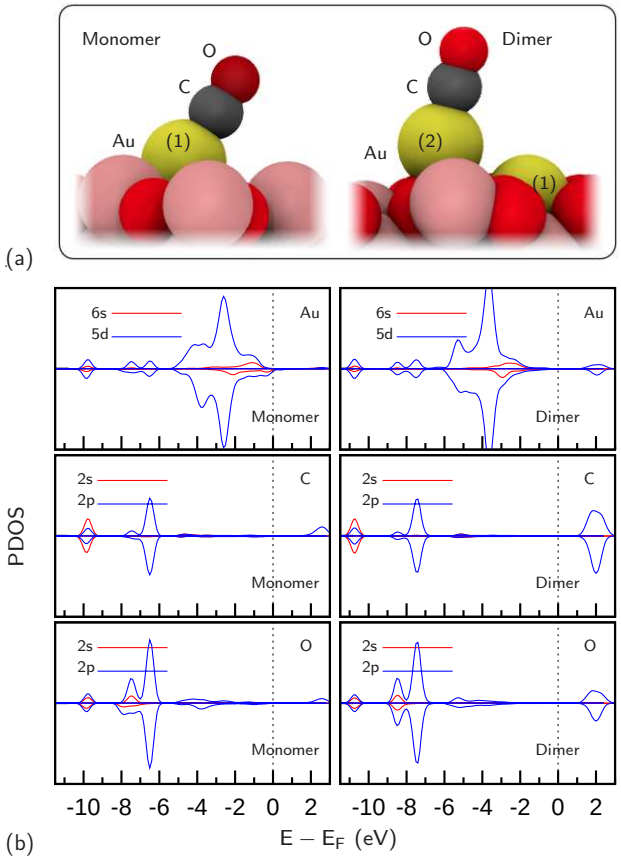

FIG. 7. (a) Adsorption geometry of CO on Au@hematite; (b) PDOS on O, C and their Au-bonding parter.

Dimer:

Fig. 6(b) shows the adsorption free energy of the CO-Au in the dimer cases. It is clear that, the V_{Fe} surface favors the CO-Au complex adsorption. In this CO-Au@V_{Fe} structure, CO strongly binds to atom Au(2) (see Table II), leading to a Au(1)-Au(2) separation of 3.15 Å which is considerably larger than its initial value of 2.64 Å. Similar to the monomer case, here the C-Au(2) bond is 1.86 Å and C-O bond is 1.15 Å. The adsorption of CO leads to the formation of an almost linear C-O-Au_1-O_s complex (O_s being a surface atom).

The binding energies of CO at $Au_{m/d}@V_{Fe}$ listed in Table II indicate that CO binds more strongly to the Au dimer than to the Au monomer. In line with this, PDOS on CO shown in Fig. 7 in both cases implies that the $2s$ and $2p$ electronic states of C, O are located at lower energy levels in the Au-dimer case compared to that in the Au-monomer case.

IV. CONCLUSION

We have studied different properties of Au monomers and dimers on the defect-free and defective terminations of an α-Fe_2O_3(0001) surface. On the basis of our density-functional calculations, we conclude that:

(i) The charge state of a Au atom adsorbed on hematite takes values between zero (metallic) to one (oxidized). Experimentally, either metallic or oxidized Au species in the Au/Fe_2O_3 systems were reported[9,11], depending on experimental conditions. In agreement with this, our calculations show a wide range of charge states of Au atoms, roughly from 0 to 1.

(ii) Au monomer adsorbed into a single Fe vacancy was identified as the most stable system (considering all the Au monomers and dimers that have been investigated in this work). Note that Au in the $Au@V_{Fe}$ system has the highest Bader charge of +1.04, because of this oxidation state, Au can formally be considered as the Au^{1+} ion. Our calculations thus show that Au replacing an Fe in the Fe_2O_3 matrix is likely the most active site for CO oxidation, as experimentally reported[9].

(iii) Single oxidized Au located at a single Fe vacancy on Fe_2O_3 results to be the thermodynamically preferred adsorption site of CO, which may serve as the oxidation site of this molecule.

* Email: manhth.nguyen@gmail.com
† Email: mfarnesi@sissa.it

[1] J. Guzman and B. C. Gates. Angew. Chem., Int. Ed. **115**, 714 (2003).
[2] J. Rodriguez, J. Evans, J. Graciani, J. B. Park, P. Liu,J. Hrbek, and J. F. Sanz. J. Phys. Chem. C **113**, 7364 (2009).
[3] D. Widmann and R. J. Behm. Acc. Chem. Res. **47**, 740 (2014).
[4] M. Haruta, N. Yamada, T. Kobayashi, and S. Iijima. J. Catal. **115**, 301 (1989).
[5] S. D. Lin, M. Bollinger, and M. A. Vannice Catal. Lett. **17**, 245 (1989).
[6] X.-Y. Wang, S.-P. Wang, S.-R. Wang, Y.-Q. Zhao, J. Huang, S.-M. Zhang, W.-P. Huang, and S.-H. Wu Catal. Lett. **112**, 115 (2006).
[7] S. K. Tanielyan and R. L. Augustine. Appl. Catal. A. **85**, 73 (1992).
[8] M. Haruta, S. Tsubota, T. Kobayashi, H. Kageyama, M. J. Genet, and B. Delmon. J. Catal. **144**, 175 (1993).
[9] S. Minico, S. Scire, C. Crisafulli, M. A. Visco, and S. Galvagno. Catal. Lett. **47**, 273 (1997).
[10] A. M. Visco, A. Donato, C. Milone, and S. Galvagno. *React.Kinet.Catal.Lett.* **61**, 219 (1997).
[11] A. M. Visco, F. Neri, G. Neri, A. Donato, C. Milone, and S. Galvagno. Phys. Chem. Chem. Phys. **1**, 2869 (1999).
[12] S. T. Daniells, A, R. Overweg, M. Makkee, and J. A. Moulijn. J. Catal. **230**, 52 (2005).
[13] B. Aeijelts Averink Silberova, M. Makkee, and J. Moulijn. Top. Catal. **44**, 209 (2007).
[14] M. A. Soria, P. Pereza, S . A. C. Carabineiro, F. J. Maldonado-Hodar, A. Mendes, and L. M. Madeir. Appl. Catal. A **470**, 45 (2014).
[15] Y.-G. Wang, Y. Yoon, V.-A. Glezakou, J. Li, and R. Rousseau. J. Am. Chem. Soc. **135**, 10673 (2013).
[16] M. F. Camellone and S. Fabris. J. Am. Chem. Soc., **131**, 10473 (2009).
[17] R. J. Lad and V. E. Henrich. Surf. Sci. **193**, 81 (1988).
[18] M.-T. Nguyen, N. Seriani, and R. Gebauer. ChemPhysChem **15**, 2930 (2014).
[19] M.-T. Nguyen, N. Seriani, and R. Gebauer. J. Chem. Phys., **138**, 194709 (2013).
[20] D. Vanderbilt. Phys. Rev. B **41**, 7892 (1990).
[21] P. Giannozzi, S. Baroni, N. Bonini, M. Calandra, R. Car, C. Cavazzoni, D. Ceresoli, G. L. Chiarotti, M. Cococcioni, I. Dabo, et al. J. Phys.:Condens. Matter **21**, 395502 (2009).
[22] J. P. Perdew, K. Burke, and M. Ernzerhof. Phys. Rev. Lett. **77**, 3865 (1996).
[23] V. I. Anisimov, J. Zaanen, and O. K. Andersen. Phys. Rev. B **44**, 943 (1991).
[24] R. F. W. Bader. W. Atoms in Molecules - A Quantum Theory (Oxford University Press, Oxford, 1990).
[25] W. Tang, E. Sanville, and G. Henkelman. J. Phys.: Condens. Matter **21**, 084204 (2009)-[http://theory.cm.utexas.edu/bader/].
[26] http://kinetics.nist.gov/janaf/
[27] K. Reuter and M. Scheffler. Phys. Rev. B. **65**, 035406 (2001).
[28] M.-T. Nguyen, N. Seriani, S. Piccinin, and R. Gebauer. J. Chem. Phys. **140**, 064703 (2014).
[29] C. Zhang, A. Michaelides, D. A. King, and S. J. Jenkins. J. Phys. Chem. C **113**, 6411 (2009).
[30] A. Kiejna and T. Pabisiak, J. Phys.: Condens. Matter , **24**, 095003 (2012).